Conflicting Interactions in Multiple Closed-Loop Controlled Critical Care Treatments: A Hemorrhage Resuscitation-Intravenous Propofol Sedation Case Study

Weidi Yin[1*], Ali Tivay[1*], George C. Kramer[2], Ramin Bighamian[3], Jin-Oh Hahn[1†]

[1]: Department of Mechanical Engineering, University of Maryland, College Park, MD 20742, USA

[2]: Department of Anesthesiology, University of Texas Medical Branch, Galveston, TX77555, USA

[3]: U.S. Food and Drug Administration, Silver Spring, MD 20903, USA

[*]Weidi Yin and Ali Tivay are equally contributing first authors.

[†]Corresponding author (e-mail: jhahn12@umd.edu)

Abstract

Closed-loop automation of critical care therapy has the potential to reduce the workload of clinical personnel while maintaining the quality of care. In the real-world clinical arena, critically ill patients receive multiple medical treatments. However, existing body of work has predominantly focused on closed-loop automation of isolated individual treatments. How these individual treatment loops interact with each other has not been investigated. The goal of this work is to garner insights on the safety of critical care therapy and potential deleterious conflicts therein when multiple isolated and individually closed-loop controlled medical treatments act upon a patient, using a case study of hemorrhage resuscitation and intravenous propofol sedation. For this purpose, a physiological model of a critically ill patient was developed and experimentally validated to describe the collective cardiovascular and pharmacological effects of these treatments. Then, isolated and individually closed-loop controlled hemorrhage resuscitation and intravenous propofol sedation treatments were simultaneously applied to the physiological model and their interactive behavior was investigated. The results showed that (i) the influence of one treatment on the other must be taken into account in selecting treatment set point to maintain the safety of overall therapy, and that (ii) information sharing between control loops may enhance the efficacy and robustness of individual treatment loops. In sum, it was concluded that hemorrhage resuscitation and intravenous propofol sedation treatments may benefit from coordination both at the set point and the loop levels. The conclusion may generalize to a wide spectrum of multiple closed-loop controlled medical treatments.

Keywords: critical care, closed-loop control, closed-loop automation, hemorrhage resuscitation, sedation, propofol

1. Introduction

Closed-loop automation of critical care therapy has the potential to reduce the workload of clinical personnel while maintaining the quality of care. Prior work suggests that caregivers have limited bandwidth to strictly titrate medical treatments to therapy goals[1,2], and that closed-loop automation may complement caregivers by automating patient monitoring and treatment titration tasks and improve the efficacy of overall therapy[3–12].

In the real-world clinical arena (such as intensive care units and emergency rooms), critically ill patients frequently receive multiple medical treatments, including hemorrhage resuscitation[13] and blood volume management[14], vasopressor therapy[15,16], sedation and analgesia[17], and mechanical ventilation[18]. Accordingly, there is a large body of existing work on the development of closed-loop automated control systems for these treatments, some of which have been evaluated in real patients to show promise[3,4,20–26,6–12,19]. However, despite the fact that these treatments must often be administered simultaneously, most prior work has predominantly focused on rather unrealistic scenarios in which an individual treatment is given in an isolated fashion. In contrast, existing work on closed-loop automation of multiple treatments simultaneously administered to a patient is relatively rare[9,12,27].

Each treatment given to a patient typically elicits changes in multiple aspects of patient physiology (including the intended change). Hence, it is to be expected that multiple closed-loop automated treatments acting on a patient may make interactions, be they synergistic or antagonistic. Taking hemorrhage resuscitation-intravenous (IV) propofol sedation as an example, (i) hemorrhage resuscitation intends to compensate for blood loss often by titrating blood volume replenishment to blood pressure (BP) while (ii) IV propofol sedation intends to sedate the patient often by titrating propofol to a depth-of-hypnosis index (e.g., BIS and WAV_{CNS}[28]). In case these treatments are administered simultaneously, they may exert conflicting effects to each other: (i) hemorrhage resuscitation increases plasma volume, dilutes plasma propofol concentration, and weakens the sedation effect of propofol; and (ii) propofol induces decrease in stressed blood volume (BV) and resistance to blood flow (called total peripheral resistance (TPR)), and thereby lowers BP. Hence, these control loops can be trapped into a vicious circle in which more volume and propofol are given indefinitely to fulfill the individual treatment goals against the antagonistic effects exerted on each other unless they are appropriately coordinated. Despite such a potential risk, closed-loop automation of multiple critical care treatments in the (rare) existing body of work has essentially stacked together isolated control loops in an ad-hoc fashion[6,9,12,29,30]. Furthermore, potentially deleterious interactions among these isolated control loops have not been extensively investigated. Hence, how individual closed-loop controlled treatments interact with each other when administered simultaneously remains unknown.

This work intends to garner insights on the safety of critical care therapy when multiple isolated and individually controlled medical treatments act upon a patient, using a case study of BP-guided hemorrhage resuscitation and BIS-guided IV propofol sedation. A physiological model of a critically ill patient to describe the collective cardiovascular (CV) and pharmacological effects of the two treatments was developed and experimentally validated. Using the physiological model, steady-state BP-BIS responses to a diverse range of resuscitation volumes and propofol infusion doses were analyzed in order to elucidate the conflicting interactions between the two treatments. Further, individually closed-loop controlled hemorrhage resuscitation and IV propofol sedation loops were applied simultaneously yet in isolation to the physiological model and their interfering

behavior was investigated under (i) a wide range of treatment set points and (ii) the presence vs. absence of information sharing between the control loops in order to demonstrate the potential benefit of control loop coordination.

2. Methods

2.1 Physiological Model of Collective Effects of Hemorrhage Resuscitation and IV Propofol Sedation

We developed a physiological model to predict the collective effects of hemorrhage resuscitation and IV propofol sedation by combining and extending a physiological model to replicate CV effects of hemorrhage and hemorrhage resuscitation developed in our prior work[31,32] and a general-purpose pharmacological model to replicate BIS effect of IV propofol[33,34] (Fig. 1). To the best of our knowledge, our physiological model is the first attempt to replicate the CV and BIS responses to combined hemorrhage resuscitation-IV propofol sedation therapy. We present a qualitative overview of the physiological model in this section. Complete mathematical details of the physiological model are given in Appendix.

The CV physiology model consists of volume kinetics in the arterial and venous vessels, vessel-tissue fluid exchange, and autonomic-cardiac regulation. The volume kinetics represents the changes in arterial and venous BV as well as BP in response to hemorrhage and hemorrhage resuscitation. The arterial and venous vessels are modeled separately as lumped compartments, with capacitance associated with each compartment relating BV and BP in the corresponding compartment. The vessel-tissue fluid exchange represents the resultant effect of the change in BV on capillary filtration and lymphatic drainage. Based on its behavior known in the literature[35], the fluid exchange is modeled phenomenologically as a dynamically regulated process to allocate total hemorrhage and resuscitation volumes to vessels and tissues. The autonomic-cardiac regulation represents the control of cardiac output (CO) and TPR to maintain arterial BP against the change in BV. Established knowledge on the CV physiology[36] is modeled into simple lumped-parameter models: (i) CO is modeled to dynamically regulate the effect of perturbation in venous BP (i.e., preload), while (ii) TPR is modeled to dynamically counteract the change in arterial BP and passively react to the change in blood viscosity.

The propofol pharmacological model consists of a 3-compartment pharmacokinetic (PK) model, an effect site delay model, and a sigmoidal pharmacodynamics (PD) model associated with BIS. We employed this PKPD model due to its adequate performance in a wide range of cohorts and clinical conditions.

In combining the CV physiology and propofol PKPD models, we made extensions to replicate the following interactions between hemorrhage resuscitation and IV propofol sedation treatments. First, we incorporated the effect of BV change on plasma propofol concentration by making the distribution volume of the central (i.e., blood) compartment in the propofol PK model (i.e., V_D in Eq. (A14)) a function of BV computed in the CV physiology model. Note that such an extension is consistent with prior experimental observations that hemorrhage and hypovolemia increases

hypnotic effect of propofol[37,38]. Second, we incorporated the arterial vasodilation and venodilation effects of propofol[39–41] by making extensions to the CV physiology model. To include the arterial vasodilation effect, we added a propofol-induced depression term to the TPR control dynamics. To include the venodilation effect, we expressed venous BV as the sum of stressed venous BV and unstressed venous BV[36], and modeled unstressed BV as a dynamical function to counteract the change in arterial BP (by way of autonomic-cardiac regulation) and passively respond to the change in plasma propofol concentration.

2.2. Model Identification and Validation

To enable realistic prediction of CV and BIS responses to hemorrhage resuscitation and propofol sedation, we estimated the parameters in the physiological model (integrating CV physiology and propofol pharmacology) using in-house experimental data and experimental results reported in the literature. Our parameter estimation was performed in two steps. First, we estimated the parameters associated with the CV physiology using in-house experimental data collected from 28 sheep (including 23 resuscitated with crystalloid and 5 resuscitated with colloid)[42–44]. In brief, the sheep underwent a major hemorrhage of 25ml/kg and received resuscitation fluid based on previously developed closed-loop control algorithms[42,44]. Using the hemorrhage and resuscitation fluid profiles as inputs and hematocrit (HCT, a well-known measure of BV[45]), CO, and arterial BP measurements as output, we formulated and solved an optimization problem with a regularization constraint[32] to estimate the CV physiology model parameters $\boldsymbol{\theta}_{\mathrm{CV}}^{*}$:

$$\boldsymbol{\theta}_{\mathrm{CV}}^{*} = \arg\min_{\boldsymbol{\theta}_{\mathrm{CV}}} \left\{ \left(\frac{1}{\sigma_{\mathrm{HCT}}} \left\| \mathbf{y}_{\mathrm{HCT}} - \hat{\mathbf{y}}_{\mathrm{HCT}}(\boldsymbol{\theta}_{\mathrm{CV}}, \mathbf{J}_{\mathrm{H}}, \mathbf{J}_{\mathrm{R}}) \right\|_2 + \frac{1}{\sigma_{\mathrm{CO}}} \left\| \mathbf{y}_{\mathrm{CO}} - \hat{\mathbf{y}}_{\mathrm{CO}}(\boldsymbol{\theta}_{\mathrm{CV}}, \mathbf{J}_{\mathrm{H}}, \mathbf{J}_{\mathrm{R}}) \right\|_2 + \frac{1}{\sigma_{\mathrm{BP}}} \left\| \mathbf{y}_{\mathrm{BP}} - \hat{\mathbf{y}}_{\mathrm{BP}}(\boldsymbol{\theta}_{\mathrm{CV}}, \mathbf{J}_{\mathrm{H}}, \mathbf{J}_{\mathrm{R}}) \right\|_2 \right) + \lambda \left\| \boldsymbol{\theta}_{\mathrm{CV}} - \boldsymbol{\theta}_{\mathrm{CV}}^{0} \right\|_1 \right\} \quad (1)$$

where $\boldsymbol{\theta}_{\mathrm{CV}}$ is the set of CV physiology model parameters defined in Appendix, $\boldsymbol{\theta}_{\mathrm{CV}}^{0}$ is the typical (population average) value of $\boldsymbol{\theta}_{\mathrm{CV}}$, $\mathbf{y}_{\mathrm{X}}$ and $\hat{\mathbf{y}}_{\mathrm{X}}$ are the vectors of measured and model-predicted physiological variable X, $\mathbf{J}_{\mathrm{H}}$ and $\mathbf{J}_{\mathrm{R}}$ are the vectors of hemorrhage and hemorrhage resuscitation profiles, σ_{HCT}, σ_{CO}, and σ_{BP} are the normalization factors, and λ is the regularization weight. The regularization term in (1) was included to achieve practical identifiability against data limitation[32]. Second, we estimated the parameters associated with the propofol pharmacology using experimental results on the CV effects of IV propofol in 17 adults[39]. In brief, the subjects received 3 different propofol infusion doses while CV responses were measured. Using the propofol infusion dose as input and CO, TPR, and arterial BP measurements as output, and assuming that the effect site time constant associated with CV endpoints is approximately twice slower than its BIS counterpart[40], we formulated and solved an optimization problem to estimate the propofol pharmacology model parameters $\boldsymbol{\theta}_{\mathrm{PD}}^{*}$:

$$\boldsymbol{\theta}_{\mathrm{PD}}^{*} = \arg\min_{\boldsymbol{\theta}_{\mathrm{PD}}} \left(\left\| \mathbf{z}_{\mathrm{CO}} - \hat{\mathbf{z}}_{\mathrm{CO}}(\boldsymbol{\theta}_{\mathrm{PD}}, \mathbf{J}_{\mathrm{P}}) \right\|_2 + \left\| \mathbf{z}_{\mathrm{TPR}} - \hat{\mathbf{z}}_{\mathrm{TPR}}(\boldsymbol{\theta}_{\mathrm{PD}}, \mathbf{J}_{\mathrm{P}}) \right\|_2 + \left\| \mathbf{z}_{\mathrm{BP}} - \hat{\mathbf{z}}_{\mathrm{BP}}(\boldsymbol{\theta}_{\mathrm{PD}}, \mathbf{J}_{\mathrm{P}}) \right\|_2 \right) \quad (2)$$

where $\boldsymbol{\theta}_{\mathrm{PD}}$ is the set of propofol PD model parameters defined in Appendix, and $\mathbf{z}_{\mathrm{X}}$ and $\hat{\mathbf{z}}_{\mathrm{X}}$ are the vectors of measured and model-predicted physiological variable X expressed in terms of its percentage change from the baseline state (corresponding to zero propofol dose). We considered

the percentage change but not the absolute change to account for the discrepancy in species between the hemorrhage/resuscitation data (sheep) and the propofol data (humans), with the implicit assumption that CV effects of propofol in terms of percentage change are comparable in sheep and humans due to the hemodynamic similarity between the two.

We investigated the validity of the physiological model using the experimental results reported in the literature not used in estimating the model parameters. First, we validated the CV physiology component of the physiological model in isolation, in terms of its ability to predict plausible CV responses to hemorrhage and hemorrhage resuscitation, by replicating the experimental results presented in 4 prior reports: (i) arterial BP, CO, and TPR responses to slow and fast crystalloid resuscitation in humans[46]; (ii) arterial BP, HCT, and CO responses to hemorrhage and crystalloid resuscitation in sheep[47]; (iii) arterial BP, fluid retention rate, and CO responses to resuscitation via crystalloid and colloid in humans[48], and (iv) arterial BP and CO responses to colloid resuscitation in humans[49]. Second, we validated the propofol PD component of the physiological model associated with the CV effects in isolation, in terms of its ability to predict plausible CV responses to propofol infusion, by replicating the experimental results presented in a prior report on arterial BP, CO, and TPR responses to IV propofol[50]. Considering that these are external validations (meaning that model parameters were not tuned specifically to these data in replicating the corresponding responses), our primary focus was to investigate the ability of the physiological model to replicate the qualitative trends of the responses in these reports.

2.3. Control Loop Interaction Analysis

Using the validated physiological model, we investigated the interactions between hemorrhage resuscitation and IV propofol sedation control loops by conducting an array of simulations. We intended to reveal the control loop interactions at two levels: (i) the set point (i.e. clinical target) level to reveal if the treatment set points must be coordinated (i.e., if the set point for one treatment must account for the set point for the other treatment), and (ii) the loop level to reveal if the control loops must be coordinated (i.e., if the control actions in one treatment must account for the control actions in the other treatment). In all the simulations conducted in this work, we used the physiological model equipped with nominal parameter values to derive generalized findings. Considering that rigorous control design is not the primary focus of this work, we empirically designed and used isolated single input-single output proportional-integral control loops for hemorrhage resuscitation and IV propofol sedation.

First, we investigated the control loop interaction at the set point level, in order to determine if the influence of hemorrhage resuscitation on BIS as well as the influence of propofol sedation on BP must be accounted for in selecting the treatment set points. To this aim, we analyzed the steady-state BP and BIS responses to a wide range of hemorrhage volumes, resuscitation volumes, and propofol infusion doses (in open-loop mode), and then (ii) performed simulations of closed-loop controlled hemorrhage resuscitation-propofol sedation therapy for diverse BP and BIS set point choices. In analyzing the steady-state responses, we considered a wide range of upper bounds associated with hourly/total resuscitation volume and propofol infusion dose to account for patient safety (note that such upper bounds are commonly employed in existing work[29]), which resulted

in a reachable BP-BIS set point region. Then, we examined the behavior of the closed-loop controlled treatments with respect to whether the treatment set points are inside or outside the reachable region by considering the following scenario (Fig. 2(a)): (i) hemorrhage was induced and was subsequently stopped; and (ii) closed-loop controlled hemorrhage resuscitation and propofol sedation were given to accomplish reachable vs. unreachable BP-BIS set points.

Second, we investigated the control loop interaction at the loop level, in order to determine if any coordination between hemorrhage resuscitation and propofol sedation control loops (e.g., alerting impending changes in resuscitation volume to propofol sedation loop and/or alerting impending changes in propofol infusion dose to hemorrhage resuscitation loop, so that individual control loops can anticipate disturbances and prepare to account for them) may enhance the efficacy and robustness of individual treatments. For this purpose, we performed simulations to examine the behavior of the closed-loop controlled treatments with respect to whether or not the impending changes in resuscitation volume and propofol infusion dose are notified to both treatment loops as alert. Our rationale is that if the therapy performance is significantly enhanced by coordination, contemporary approach to closed-loop controlled critical care therapy (multiple single input-single output control loops isolated from one another) must ideally be replaced by more sophisticated yet interactive multivariable control loops. To examine the advantage of alerting propofol infusion dose change to hemorrhage resuscitation, we considered the following scenario: (i) hemorrhage was induced and was subsequently stopped; (ii) closed-loop controlled hemorrhage resuscitation and propofol sedation were given to accomplish a reachable BP-BIS set point; and (iii) BIS set point was decreased by a stepwise increase in the propofol infusion dose while BP set point was maintained (Fig. 2(b)). Then, we compared the transient BP-BIS response in the absence vs. presence of alert: (i) in the absence of alert, the hemorrhage resuscitation control loop operated solely based on the BP measurement independently of the propofol sedation control loop; while (ii) in the presence of alert, the hemorrhage resuscitation control loop administered extra bolus volume required to counteract the BP-lowering effect of the change in the BIS set point in the steady state (note that this required volume can be readily computed based on the steady-state analysis mentioned above). To examine the advantage of alerting resuscitation volume change to propofol sedation, we considered the following scenario: (i) hemorrhage was induced and was subsequently stopped; (ii) closed-loop controlled hemorrhage resuscitation and propofol sedation were given to accomplish a reachable BP-BIS set point; and (iii) BP set point was increased via a resuscitation bolus while BIS set point was maintained (Fig. 2(c)). Then, we likewise compared the transient BP-BIS response in the absence vs. presence of alert: (i) in the absence of alert, the propofol sedation control loop operated solely based on the BIS measurement independently of the hemorrhage resuscitation control loop; while (ii) in the presence of alert, the propofol sedation control loop made a stepwise increase in the infusion dose required to counteract the BIS-raising effect of the change in BP set point in the steady state (note that this required infusion dose can be readily computed based on the steady-state analysis mentioned above). In both scenarios, we varied hemorrhage volume as well as BP-BIS set points widely to garner insights on the control loop behavior as well as to ascertain its robust generalizability.

3. Results

Table 1 summarizes the goodness of fit results obtained from the internal validations conducted for the physiological model in terms of normalized root-mean-squared error. Fig. 3 presents the results obtained from the external validations conducted for the physiological model. Table 2 summarizes both transient and steady-state effects made by the crystalloid/colloid bolus and propofol (at a constant infusion dose) on CV variables and BIS. Fig. 4 presents the representative examples of reachable BP-BIS set point region in the steady state pertaining to (a) crystalloid-propofol and (b) colloid-propofol, associated with 0.75 L hemorrhage volume as well as 1.5 L total resuscitation volume and 0.25 mcg/kg/min propofol infusion dose (amounting to BIS=30 in the steady state at the pre-resuscitation BV level) as therapeutic upper bounds. Fig. 5 presents BP-BIS and CO-TPR phase plots comparing the dynamic behavior of the closed-loop controlled colloid-based hemorrhage resuscitation and propofol sedation treatments commanded to track representative set points in the (a) reachable region, (b) region pertaining to volume (i.e., colloid) overload, and (c) region pertaining to propofol over-dosing in Fig. 4. Fig. 6 shows BP-BIS phase plots comparing the transient set point tracking behavior of the closed-loop controlled hemorrhage resuscitation-propofol sedation treatments in the absence vs. presence of alert (i.e., information sharing) between the two control loops: (a) hemorrhage resuscitation with vs. without BIS set point change alert and (b) propofol sedation with vs. without hemorrhage resuscitation set point change alert.

4. Discussion

Closed-loop automation of critical care therapy is gaining an increasing interest both in research and clinical domains as a means to reduce the workload of clinical personnel while maintaining the quality of care. Critically ill patients frequently receive multiple medical treatments. However, closed-loop automation of individual critical care treatments in an isolated setting has been the mainstay of existing body of work, with no explicit account for (potentially conflicting) interactions among multiple treatment control loops. In our attempt to make a paradigm shift, we intended to garner insights on the safety of critical care therapy and potential conflicts therein when multiple isolated and individually controlled medical treatment loops act upon a patient. To this aim, we used a case study of hemorrhage resuscitation and IV propofol sedation. We demonstrated that (i) the safety of critical care therapy consisting of multiple closed-loop controlled treatments may be deteriorated if the treatment set points are chosen without taking the interactions among the treatments into account, and that (i) the efficacy and robustness of multiple closed-loop controlled treatments may be enhanced by allowing the control loops to communicate and share information with one another. Details follow.

4.1. Validity of Physiological Model

Internal validation of the physiological model suggested that the optimization problems in Eq. (1)-(2) were adequately solved to yield small cost function values, and that the physiological model equipped with appropriate parameter values can predict physiologically plausible BV, CO, and arterial BP responses to hemorrhage and hemorrhage resuscitation as well as propofol sedation. Indeed, the physiological model exhibited reasonable goodness of fit with respect to the data used

in Eq. (1) with normalized root-mean-squared errors consistently smaller than 12% in HCT, CO, and arterial BP, and also with respect to the data used in Eq. (2) with normalized root-mean-squared errors consistently smaller than 5% in CO, TPR, and arterial BP.

External validation of the physiological model demonstrated great promise. First, it could replicate the qualitative trend of arterial BP, CO, and TPR responses to hemorrhage as well as slow and fast crystalloid resuscitation, including (i) minimal arterial BP change and (ii) large changes in CO and TPR (relative to BP) in correct directions and magnitudes in response to hemorrhage (T_2) and crystalloid resuscitation (T_3-T_6) (Fig. 3(a)), and additionally, (iii) drastic decrease in BV in response to hemorrhage and its incomplete recovery to the pre-hemorrhagic level in response to resuscitation (not shown). Second, it could replicate the qualitative trend of arterial BP, HCT, and CO responses to crystalloid resuscitation after hemorrhage, including (i) large decrease in arterial BP and CO in response to hemorrhage (T_2), (ii) temporary recovery in arterial BP and CO in response to crystalloid resuscitation (T_3) and ultimate convergence to sub-pre-hemorrhagic levels (T_4), and (iii) monotonic decrease in HCT (Fig. 3(b)). Third, it could replicate the qualitative trend of arterial BP, fluid retention rate, and CO responses to crystalloid and colloid administration, especially the pronounced increases in these responses to colloid relative to crystalloid (Fig. 3(c)). Fourth, it could replicate the qualitative trend of arterial BP and CO responses to colloid (Fig. 3(d)). Fifth, it could replicate the qualitative trend of arterial BP, CO, and TPR responses to IV propofol administration, including (i) decrease in CO (due to venodilation decreasing stressed BV) and TPR (due to arterial vasodilation), and as a consequence, (ii) decrease in arterial BP (Fig. 3(e)). In addition to the abovementioned qualitative trends, the physiological model could even adequately predict the quantitative trends in all the external validations in Fig. 3. Considering that the external validation was performed without any tuning of the model parameters beyond the optimization trials performed in (1)-(2), the results demonstrate that the physiological model boasts reasonable predictive capability to enable extensive analysis of the dynamic interactions occurring between closed-loop controlled hemorrhage resuscitation and propofol sedation treatments.

4.2. Conflicting Interactions in Closed-Loop Controlled Hemorrhage Resuscitation and IV Propofol Sedation

The results derived from the control loop interaction analysis for hemorrhage resuscitation and IV propofol sedation treatments (Section 2.3) illustrate that coordination may be desired both at the set point level and loop level in order to de-conflict the two treatments. At the set point level, BP and BIS set points given to hemorrhage resuscitation and IV propofol sedation control loops must account for the influence of one treatment to the other to ensure the safety of the overall therapy. Hemorrhage resuscitation and propofol sedation exert conflicting effects on BP and BIS especially in case of colloid resuscitation (Table 1 and Fig. 4): (i) administering crystalloid/colloid to raise BP also raises BIS (meaning it lowers the depth of sedation) by diluting propofol in the blood and thus lowering the plasma propofol concentration, and (ii) increasing the propofol infusion dose to lower BIS also lowers BP by lowering TPR and stressed BV. It may be naively anticipated that closed-loop control algorithms for hemorrhage resuscitation and propofol sedation may compensate for such excursions in the controlled variables by suppressing the disturbances originating from such

a conflicting treatment. However, the ability of the closed-loop control algorithms to compensate for such excursions hinges upon the restrictions given to the allowed (hourly/total) resuscitation volume and propofol infusion dose, viewed as the actuator saturation in the control community. More specifically, a BP-BIS set point can be achieved if it is in the reachable region determined by the upper bounds of resuscitation volume and propofol infusion does (i.e., actuator saturation) ((A) in Fig. 4(b)). In contrast, it cannot be achieved if it is outside the reachable region (meaning that BP set point is too high and/or BIS set point is too low), or in the absence of actuator saturation, may be reached at the cost of unacceptable resuscitation volume and propofol infusion dose ((B), (C), and (B)+(C) in Fig. 4(b)). Fig. 5 corroborates convincing supports to our claim: (i) closed-loop controlled therapy can achieve a set point in the reachable region (Fig. 5(a)), but (ii) it either fails to achieve a set point (when actuator saturation is enforced) or leads to unacceptable CO and TPR values in the patient (when actuator saturation is relaxed) if the set point is outside the reachable region (Fig. 5(b)) and Fig. 5(c)). In Fig. 5(b), the set point is in the volume overload region ((B)) in Fig. 4(b). Hence, BIS set point is achieved while BP set point is not achieved if the actuator saturation is in effect. In Fig. 5(c), the set point is in the propofol over-dosing region ((C)) in Fig. 4(b). Hence, BP set point is achieved while BIS set point is not achieved if the actuator saturation is in effect. In both cases, to achieve the selected set points required massive colloid volume resuscitation and propofol infusion dose, resulting in physiologically unacceptable level of CO and TPR (see the blue solid traces in Fig. 5(b) and Fig. 5(c)). Therefore, the results indicate that BP-BIS set points must be coordinated to ensure that it resides in the reachable region to guarantee patient safety.

Comparing the reachable regions associated with crystalloid (Fig. 4(a)) and colloid (Fig. 4(b)), the region is much smaller in the case of crystalloid than colloid. Hence, simultaneous administration of hemorrhage resuscitation and propofol sedation with BP and BIS as controlled variables may present more significant challenges in the case of crystalloid than colloid. Specifically, crystalloid has minimal effect on BP (which is consistent with existing experimental reports; see, e.g., Fig. 3(a) and Fig. 3(c)). Hence, BP set point associated with crystalloid resuscitation must be raised (or lowered) if BIS set point is to be raised (or lowered). Fluid overload may result otherwise. Despite to a moderate extent, BP-BIS set point must likewise be chosen in coordination in case of colloid resuscitation: (i) BP set point must be properly raised (or lowered) if BIS set point is to be raised (or lowered), and (ii) BIS set point must be properly raised (or lowered) if BP set point is to be raised (or lowered).

At the loop level, the efficacy, robustness, and safety of individual treatment control loops may be enhanced by sharing information on the operation of individual control loops. For example, Fig. 6 demonstrates that the transient set point tracking behavior may be largely improved if set point change information is shared between hemorrhage resuscitation and propofol sedation control loops, by enabling each control loop to “look ahead and reconcile” the impending disturbance due to the set point change in the other control loop rather than forcing it to “react” to the disturbance once it is sensed through the excursions in the controlled variables. Indeed, the excursion in BP could be reduced significantly when the hemorrhage control loop was informed of the change in the propofol infusion dose (to deepen sedation) in advance (Fig. 6(a)). Such a robustness in BP regulation may contribute to the prevention of potentially dangerous hypotension. In addition, the excursion in BIS could be likewise reduced when the propofol sedation control loop was informed

of the change in the resuscitation volume (to raise BP and improve hemodynamics, be it a bolus or an infusion) in advance (Fig. 6(b)). It is noted that the excursion in BIS in Fig. 6(b) was not substantial in absolute amount. However, the excursion can be exacerbated in real-world clinical scenarios, e.g., in case resuscitation volume is given while surgical stimulation is applied (which is known to increase BIS[51,52]). In addition, Fig. 5(a) illustrates another aspect of potential benefit associated with coordination at the loop level: hemorrhage resuscitation and propofol sedation control loops can be reconciled to make an optimal set point transition (e.g., to follow the "ideal path" in Fig. 5(a)) to prevent unnecessary overshoot and undershoot in BP and BIS. Considering the advantage garnered by simply alerting the set point change to the other treatment control loop in conjunction with ad-hoc yet preventive disturbance rejection action shown in Fig. 6, we contend that more sophisticated multivariable control techniques may have the potential to make more significant enhancements in the transient behavior of the control loops. Indeed, multivariable control design techniques may provide systematic means to incorporate the physiological and pharmacological mechanisms underlying the interaction between hemorrhage resuscitation and propofol sedation treatments into the development of closed-loop control algorithms capable of autonomously reconciling multiple treatment goals by exploiting the physiological model in the control design process.

In summary, our work demonstrates that control loop coordination is desired both at the set point level and at the loop level to de-conflict the closed-loop controlled hemorrhage resuscitation and propofol sedation treatments, motivating the rigorous investigation of autonomous multivariable set point selection for and closed-loop control of multiple critical care treatments.

4.3. Generalization to Diverse Critical Care Treatments

In this work, we focused on the analysis of conflicting interference between closed-loop controlled hemorrhage resuscitation and propofol sedation treatments. However, the analysis framework presented in this work may be easily generalized to investigate possible interference between diverse critical care treatments of interest. One such treatment of practical significance may be mechanical ventilation. It is known that mechanical ventilation tends to decrease the sensitivity of autonomic-cardiac regulation during general anesthesia[41]. Hence, mechanical ventilation will introduce an additional dimension in the analysis of conflicting interference between hemorrhage resuscitation and propofol sedation by making alterations to vasodilation and venodilation effects of propofol. Such a complex interactions may still be readily elucidated by extending the analysis performed in this work, by incorporating a physiological model of breathing with mechanically ventilation into the physiological model presented in this work and its influences on CV responses. The analysis framework presented in this work may likewise be easily generalized to investigate closed-loop controlled critical care treatments based on diverse endpoints. For example, this work used arterial BP as the endpoint for hemorrhage resuscitation. However, other endpoints, including pulse pressure variability[53] (which is a predictor of BV) and variabilities associated with autonomic cardiac regulation[54] (which are associated with mortality), may be accommodated in the analysis framework by, e.g., extending the physiological model presented in this work to the one in which systolic, mean, and diastolic BP levels can be predicted, or even to the one in which arterial BP waveform itself can be predicted[55]. In sum, with the

availability of physiological models suited to the intended analysis (which may be furnished by extending the physiological model presented in this work), this work may provide a potentially powerful framework for elucidating and developing solutions to resolve therapeutic safety concerns due to conflicting interference between multiple closed-loop controlled critical care treatments.

5. Conclusion and Future Work

This work demonstrated the potential of destructive interference between individually closed-loop controlled hemorrhage resuscitation and IV propofol sedation treatments in critically ill patients. It was illustrated that efficacy and safety of the overall therapy are degraded if treatment set points are selected without careful account for the conflicting CV and pharmacological effects of the two treatments and/or if treatment information is not shared between the two control loops. Findings made in this work suggest opportunities for coordination of closed-loop hemorrhage resuscitation and IV propofol sedation control loops both at the set point and loop levels, and may generalize to many closed-loop controlled critical care treatments administered simultaneously. Future work must invest effort to develop systematic and scalable solutions that can enable safety-preserving coordination of interacting closed-loop controlled treatment loops in the critical care arena.

Funding

This work was supported by the U.S. Office of Naval Research (ONR) (Grant No. N00014-19-1-2402), the U.S. National Science Foundation (NSF) CAREER Award (Grant No. CNS-1748762), and the Congressionally Directed Medical Research Programs (Grant No. W81XWH-19-1-0322).

Disclaimer

This article reflects the views of the authors and should not be construed to represent FDA's views or policies.

References

[1] G. Hawryluk, W. Whetstone, R. Saigal, A. Ferguson, J. Talbott, J. Bresnahan, S. Dhall, J. Pan, M. Beattie, G. Manley, Mean Arterial Blood Pressure Correlates with Neurological Recovery after Human Spinal Cord Injury: Analysis of High Frequency Physiologic Data, J. Neurotrauma. 32 (2015) 1958–1967. https://doi.org/10.1089/neu.2014.3778.

[2] B. Yapps, S. Shin, R. Bighamian, J. Thorsen, C. Arsenault, S.A. Quraishi, J.-O. Hahn, A.T. Reisner, Hypotension in ICU Patients Receiving Vasopressor Therapy, Sci. Rep. 7 (2017) 8551. https://doi.org/10.1038/s41598-017-08137-0.

[3] J. Rinehart, M. Lilot, C. Lee, A. Joosten, T. Huynh, C. Canales, D. Imagawa, A. Demirjian, M. Cannesson, Closed-Loop Assisted versus Manual Goal-Directed Fluid Therapy during High-Risk Abdominal Surgery: A Case-Control Study with Propensity Matching, Crit. Care.

19 (2015) 94. https://doi.org/10.1186/s13054-015-0827-7.

[4] J. Rinehart, C. Lee, C. Canales, A. Kong, Z. Kain, M. Cannesson, Closed-Loop Fluid Administration Compared to Anesthesiologist Management for Hemodynamic Optimization and Resuscitation during Surgery: An In Vivo Study, Anesth. Analg. 117 (2013) 1119–1129. https://doi.org/10.1213/ANE.0b013e3182937d61.

[5] S.L. Hoskins, G.I. Elgjo, J. Lu, H. Ying, J.J. Grady, D.N. Herndon, G.C. Kramer, Closed-Loop Resuscitation of Burn Shock, J. Burn Care Res. 27 (2006) 377–385. https://doi.org/10.1097/01.BCR.0000216512.30415.78.

[6] B.L. Sng, H.S. Tan, a. T.H. Sia, Closed-Loop Double-Vasopressor Automated System vs Manual Bolus Vasopressor to Treat Hypotension during Spinal Anaesthesia for Caesarean Section: A Randomised Controlled Trial, Anaesthesia. 69 (2014) 37–45. https://doi.org/10.1111/anae.12460.

[7] T.M. Hemmerling, S. Charabati, C. Zaouter, C. Minardi, P.A. Mathieu, A Randomized Controlled Trial Demonstrates that A Novel Closed-Loop Propofol System Performs Better Hypnosis Control than Manual Administration, Can. J. Anesth. 57 (2010) 725–735. https://doi.org/10.1007/s12630-010-9335-z.

[8] J. Agarwal, G.D. Puri, P.J. Mathew, Comparison of Closed Loop vs. Manual Administration of Propofol using the Bispectral Index in Cardiac Surgery, Acta Anaesthesiol. Scand. 53 (2009) 390–397. https://doi.org/10.1111/j.1399-6576.2008.01884.x.

[9] N. Liu, T. Chazot, S. Hamada, A. Landais, N. Boichut, C. Dussaussoy, B. Trillat, L. Beydon, E. Samain, D.I. Sessler, M. Fischler, Closed-Loop Coadministration of Propofol and Remifentanil Guided by Bispectral Index: A Randomized Multicenter Study, Anesth. Analg. 112 (2011) 546–557. https://doi.org/10.1213/ANE.0b013e318205680b.

[10] L. Pasin, P. Nardelli, M. Pintaudi, M. Greco, M. Zambon, L. Cabrini, A. Zangrillo, Closed-Loop Delivery Systems Versus Manually Controlled Administration of Total IV Anesthesia, Anesth. Analg. 124 (2017) 456–464. https://doi.org/10.1213/ANE.0000000000001394.

[11] N. Liu, T. Chazot, A. Genty, A. Landais, A. Restoux, K. McGee, P.A. Laloë, B. Trillat, L. Barvais, M. Fischler, Titration of Propofol for Anesthetic Induction and Maintenance Guided by the Bispectral Index: Closed-Loop versus Manual Control: A Prospective, Randomized, Multicenter Study, Anesthesiology. 104 (2006) 686–695. https://doi.org/10.1097/00000542-200604000-00012.

[12] C. Dussaussoy, M. Peres, V. Jaoul, N. Liu, T. Chazot, J. Picquet, M. Fischler, L. Beydon, Automated Titration of Propofol and Remifentanil Decreases the Anesthesiologist's Workload during Vascular or Thoracic Surgery: A Randomized Prospective Study, J. Clin. Monit. Comput. 28 (2014) 35–40. https://doi.org/10.1007/s10877-013-9453-6.

[13] A. Bouglé, A. Harrois, J. Duranteau, Resuscitative Strategies in Traumatic Hemorrhagic Shock, Ann. Intensive Care. 3 (2013) 1. https://doi.org/10.1186/2110-5820-3-1.

[14] L.H. Camacho Navarro, J.A. Bloomstone, O.J. Costa Auler, M. Cannesson, G. Della Rocca, T.J. Gan, M. Kinsky, S. Magder, T.E. Miller, M. Mythen, A. Perel, D.A. Reuter, M.R. Pinsky, G.C. Kramer, Perioperative Fluid Therapy: A Statement from the International Fluid Optimization Group, Perioper. Med. 4 (2015) Article 3. https://doi.org/10.1186/s13741-015-0014-z.

[15] T.J. Ellender, J.C. Skinner, The Use of Vasopressors and Inotropes in the Emergency

Medical Treatment of Shock, Emerg. Med. Clin. North Am. 26 (2008) 759–786. https://doi.org/10.1016/j.emc.2008.04.001.

[16] M.N. Bangash, M.-L. Kong, R.M. Pearse, Use of Inotropes and Vasopressor Agents in Critically Ill Patients, Br. J. Pharmacol. 165 (2012) 2015–2033. https://doi.org/10.1111/j.1476-5381.2011.01588.x.

[17] J. Rinehart, N. Liu, B. Alexander, M. Cannesson, Closed-Loop Systems in Anesthesia: Is There a Potential for Closed-Loop Fluid Management and Hemodynamic Optimization?, Anesth. Analg. 114 (2012) 130–143. https://doi.org/10.1213/ANE.0b013e318230e9e0.

[18] F. Fichtner, O. Mörer, S. Laudi, S. Weber-Carstens, M. Nothacker, U. Kaisers, Clinical Practice Guideline: Mechanical ventilation and Extracorporeal Membrane Oxygenation in Acute Respiratory Insufficiency, Dtsch. Arztebl. Int. 115 (2018) 840–847. https://doi.org/10.3238/arztebl.2018.0840.

[19] F.C. Jandre, A. V. Pino, I. Lacorte, J.H.S. Neves, A. Giannella-Neto, A Closed-Loop Mechanical Ventilation Controller with Explicit Objective Functions, IEEE Trans. Biomed. Eng. 51 (2004) 823–831. https://doi.org/10.1109/TBME.2004.826678.

[20] F. Lellouche, L. Brochard, Advanced Closed Loops during Mechanical Ventilation (PAV, NAVA, ASV, SmartCare), Best Pract. Res. Clin. Anaesthesiol. 23 (2009) 81–93. https://doi.org/10.1016/j.bpa.2008.08.001.

[21] R.L. Chatburn, R. Faarc, Computer Control of Mechanical Ventilation, Respir. Care. 49 (2004) 507–515.

[22] T. Nemoto, G.E. Hatzakis, C.W. Thorpe, R. Olivenstein, S. Dial, J.H. Bates, Automatic Control of Pressure Support Mechanical Ventilation using Fuzzy Logic, Am. J. Respir. Crit. Care Med. 160 (1999) 550–556. https://doi.org/10.1164/ajrccm.160.2.9809013.

[23] D.M. Linton, P.D. Potgieter, S. Davis, A.T.J. Fourie, J.X. Brunner, T.P. Laubscher, Automatic Weaning from Mechanical Ventilation using an Adaptive Lung Ventilation Controller, Chest. 106 (1994) 1843–1850. https://doi.org/10.1378/chest.106.6.1843.

[24] J. Schäublin, M. Derighetti, P. Feigenwinter, S. Petersen-Felix, A.M. Zbinden, Fuzzy Logic Control of Mechanical Ventilation during Anaesthesia, Br. J. Anaesth. 77 (1996) 636–641.

[25] E.P. Martinoni, C.A. Pfister, K.S. Stadler, P.M. Schumacher, D. Leibundgut, T. Bouillon, T. Böhlen, A.M. Zbinden, Model-Based Control of Mechanical Ventilation: Design and Clinical Validation, Br. J. Anaesth. 92 (2004) 800–807. https://doi.org/10.1093/bja/aeh145.

[26] H. Jin-Oh, G.A. Dumont, J.M. Ansermino, System Identification and Closed-Loop Control of End-Tidal CO2 in Mechanically Ventilated Patients, IEEE Trans. Inf. Technol. Biomed. 16 (2012) 1176–1184. https://doi.org/10.1109/titb.2012.2204067.

[27] X. Jin, C.-S. Kim, S.T. Shipley, G.A. Dumont, J.-O. Hahn, Coordinated Semi-Adaptive Closed-Loop Control for Infusion of Two Interacting Medications, Int. J. Adapt. Control Signal Process. 32 (2018) 134–146. https://doi.org/10.1002/acs.2832.

[28] S. Bibian, G.A. Dumont, T. Zikov, Dynamic Behavior of BIS, M-Entropy and NeuroSENSE Brain Function Monitors, J. Clin. Monit. Comput. 25 (2011) 81–87. https://doi.org/10.1007/s10877-010-9266-9.

[29] A. Joosten, V. Jame, B. Alexander, T. Chazot, N. Liu, M. Cannesson, J. Rinehart, L. Barvais, Feasibility of Fully Automated Hypnosis, Analgesia, and Fluid Management Using

2 Independent Closed-Loop Systems during Major Vascular Surgery: A Pilot Study, Anesth. Analg. 128 (2019) E88–E92. https://doi.org/10.1213/ANE.0000000000003433.

[30] F. Tehrani, M. Rogers, T. Lo, T. Malinowski, S. Afuwape, M. Lum, B. Grundl, M.S. Terry, A Dual Closed-Loop Control System for Mechanical Ventilation, J. Clin. Monit. Comput. 18 (2004) 111–129.

[31] A. Tivay, G.C. Kramer, J.-O. Hahn, Virtual Patient Generation using Physiological Models through a Compressed Latent Parameterization, in: Proc. 2020 Am. Control Conf., Denver, CO, USA, 2020. https://doi.org/10.23919/ACC45564.2020.914729.

[32] A. Tivay, X. Jin, A. Lo, C.G. Scully, J.-O. Hahn, Practical Use of Regularization in Individualizing a Mathematical Model of Cardiovascular Hemodynamics Using Scarce Data, Front. Physiol. 11 (2020) Article 452. https://doi.org/10.3389/fphys.2020.00452.

[33] D.J. Eleveld, J.H. Proost, L.I. Cortínez, A.R. Absalom, M.M.R.F. Struys, A General Purpose Pharmacokinetic Model for Propofol, Anesth. Analg. 118 (2014) 1221–1237. https://doi.org/10.1213/ANE.0000000000000165.

[34] D.J. Eleveld, P. Colin, A.R. Absalom, M.M.R.F. Struys, Pharmacokinetic–Pharmacodynamic Model for Propofol for Broad Application in Anaesthesia and Sedation, Br. J. Anaesth. 120 (2018) 942–959. https://doi.org/10.1016/j.bja.2018.01.018.

[35] A.C. Guyton, A.E. Taylor, H.J. Granger, Circulatory Physiology II: Dynamics and Control of the Body Fluids, W.B. Saunders Company, 1975.

[36] L.S. Costanzo, Physiology, Lippincott Williams & Wilkins, Philadelphia, PA, 2011.

[37] P. De Paepe, F.M. Belpaire, G. Van Hoey, P.A. Boon, W.A. Buylaert, The Influence of Hypovolemia on the Pharmacokinetics and the Electroencephalographic Effect of Propofol in the Rat, Anesthesiology. 93 (2000) 1482–1490. https://doi.org/10.1002/jps.10275.

[38] T. Kurita, K. Takata, K. Morita, Y. Morishima, M. Uraoka, T. Katoh, S. Sato, The Influence of Hemorrhagic Shock on the Electroencephalographic and Immobilizing Effects of Propofol in a Swine Model, Anesth. Analg. 109 (2009) 398–404. https://doi.org/10.1213/ane.0b013e3181a96f9a.

[39] F. De Wit, A.L. Van Vliet, R.B. De Wilde, J.R. Jansen, J. Vuyk, L.P. Aarts, E. De Jonge, D.P. Veelo, B.F. Geerts, The Effect of Propofol on Haemodynamics: Cardiac Output, Venous Return, Mean Systemic Filling Pressure, and Vascular Resistances, Br. J. Anaesth. 116 (2016) 784–789. https://doi.org/10.1093/bja/aew126.

[40] M.M. Sahinovic, M.M.R.F. Struys, A.R. Absalom, Clinical Pharmacokinetics and Pharmacodynamics of Propofol, Clin. Pharmacokinet. 57 (2018) 1539–1558. https://doi.org/10.1007/s40262-018-0672-3.

[41] A. Porta, V. Bari, T. Bassani, A. Marchi, V. Pistuddi, M. Ranucci, Model-Based Causal Closed-Loop Approach to the Estimate of Baroreflex Sensitivity during Propofol Anesthesia in Patients Undergoing Coronary Artery Bypass Graft, J. Appl. Physiol. 115 (2013) 1032–1042. https://doi.org/10.1152/japplphysiol.00537.2013.

[42] A.D. Rafie, P.A. Rath, M.W. Michell, R.A. Kirschner, D.J. Deyo, D.S. Prough, J.J. Grady, G.C. Kramer, Hypotensive Resuscitation of Multiple Hemorrhages using Crystalloid and Colloids, Shock. 22 (2004) 262–269. https://doi.org/10.1097/01.shk.0000135255.59817.8c.

[43] S.U. Vaid, A. Shah, M.W. Michell, A.D. Rafie, D.J. Deyo, D.S. Prough, G.C. Kramer,

Normotensive and Hypotensive Closed-Loop Resuscitation using 3.0% NaCl to Treat Multiple Hemorrhages in Sheep, Crit. Care Med. 34 (2006) 1185–1192. https://doi.org/10.1097/01.CCM.0000207341.78696.3A.

[44] N.R. Marques, B.J. Ford, M.N. Khan, M. Kinsky, D.J. Deyo, W.J. Mileski, H. Ying, G.C. Kramer, Automated Closed-Loop Resuscitation of Multiple Hemorrhages: A Comparison between Fuzzy Logic and Decision Table Controllers in a Sheep Model, Disaster Mil. Med. 3 (2017) 1. https://doi.org/10.1186/s40696-016-0029-0.

[45] R.G. Hahn, Volume Kinetics for Infusion Fluids, Anesthesiology. 113 (2010) 470–481.

[46] L. Ho, L. Lau, L. Churilov, B. Riedel, L. Mcnicol, R.G. Hahn, L. Weinberg, Comparative Evaluation of Crystalloid Resuscitation Rate in a Human Model of Compensated Haemorrhagic Shock, Shock. 46 (2016) 149–157. https://doi.org/10.1097/SHK.0000000000000610.

[47] S.R. Fischer, M. Burnet, D.L. Traber, D.S. Prough, G.C. Kramer, Plasma Volume Expansion with Solutions of Hemoglobin, Albumin and Ringer's Lactate in Sheep, Crit. Care Med. 276 (1999) H2194–H2203. https://doi.org/10.1097/00003246-199901001-00518.

[48] S. Sondergaard, J.S. Larsson, P.W. Möller, The Haemodynamic Effects of Crystalloid and Colloid Volume Resuscitation on Primary, Derived and Efficiency Variables in Post-CABG Patients, Intensive Care Med. Exp. 7 (2019) 13. https://doi.org/10.1186/s40635-019-0224-7.

[49] Y. Le Manach, C.K. Hofer, J.J. Lehot, B. Vallet, J.P. Goarin, B. Tavernier, M. Cannesson, Can Changes in Arterial Pressure Be Used to Detect Changes in Cardiac Output during Volume Expansion in the Perioperative Period?, Anesthesiology. 117 (2012) 1165–1174. https://doi.org/10.1097/ALN.0b013e318275561d.

[50] D. Aditianingsih, B. Sukmono, T.A. Agung, W.Y. Kartolo, E.S. Adiwongso, C.A. Mochtar, Comparison of the Effects of Target-Controlled Infusion of Propofol and Sevoflurane as Maintenance of Anesthesia on Hemodynamic Profile in Kidney Transplantation, Anesthesiol. Res. Pract. 2019 (2019) Article 5629371. https://doi.org/10.1155/2019/5629371.

[51] K. Soltesz, J.O. Hahn, T. Hägglund, G. a. Dumont, J.M. Ansermino, Individualized Closed-Loop Control of Propofol Anesthesia: A Preliminary Study, Biomed. Signal Process. Control. 8 (2013) 500–508. https://doi.org/10.1016/j.bspc.2013.04.005.

[52] J.O. Hahn, G. a. Dumont, J.M. Ansermino, Robust Closed-Loop Control of Hypnosis with Propofol using WAV_CNS Index as the Controlled Variable, Biomed. Signal Process. Control. 7 (2012) 517–524. https://doi.org/10.1016/j.bspc.2011.09.001.

[53] M. Cannesson, M. Aboy, C.K. Hofer, M. Rehman, Pulse Pressure Variation: Where Are We Today?, J. Clin. Monit. Comput. 25 (2011) 45–56. https://doi.org/10.1007/s10877-010-9229-1.

[54] A. Porta, R. Colombo, A. Marchi, V. Bari, B. De Maria, G. Ranuzzi, S. Guzzetti, T. Fossali, F. Raimondi, Association between Autonomic Control Indexes and Mortality in Subjects Admitted to Intensive Care Unit, Sci. Rep. 8 (2018) 1–13. https://doi.org/10.1038/s41598-018-21888-8.

[55] M. Ursino, Interaction between Carotid Baroregulation and the Pulsating Heart: A

Mathematical Model, Am. J. Physiol. 275 (1998) H1733–H1747.

[56] R. Bighamian, A.T. Reisner, J. Hahn, A Lumped-Parameter Subject-Specific Model of Blood Volume Response to Fluid Infusion, Front. Physiol. 7 (2016) 390. https://doi.org/10.3389/fphys.2016.00390.

[57] R. Bighamian, B. Parvinian, C.G. Scully, G.C. Kramer, J.-O. Hahn, Control-Oriented Physiological Modeling of Hemodynamic Responses to Blood Volume Perturbation, Control Eng. Pract. (2018).

[58] R. Bighamian, M. Kinsky, G. Kramer, J.-O. Hahn, In-Human Subject-Specific Evaluation of a Control-Theoretic Plasma Volume Regulation Model, Comput. Biol. Med. 91 (2017) 96–102. https://doi.org/10.1016/j.compbiomed.2017.10.006.

Appendix: Physiological Model of Collective Effects of Hemorrhage Resuscitation and IV Sedation

The CV physiology model consists of volume kinetics in the arterial and venous vessels, vessel-tissue fluid exchange, and autonomic-cardiac regulation. Details and complete set of equations are presented below.

A.1. Volume Kinetics

The volume kinetics represent changes in arterial and venous BV and BP in response to blood gain and loss. The arterial and venous vessels are modeled separately as lumped compartments subject to blood gain and loss as well as blood flow between them (Fig. 1):

$$\dot{V}_A(t) = Q(t) - \frac{P_A(t)-P_V(t)}{R(t)} - J_H(t) - J_E(t) \quad \text{(A1)}$$

$$\dot{V}_V(t) = -Q(t) + \frac{P_A(t)-P_V(t)}{R(t)} + J_R(t) \quad \text{(A2)}$$

$$\dot{V}_{RBC}(t) = -J_H(t)\frac{V_{RBC}(t)}{V_A(t)+V_V(t)} \quad \text{(A3)}$$

where V_A, V_V, and V_{RBC} are arterial and venous BV as well as red blood cell (RBC) volume, Q is CO, R is TPR, P_A and P_V are arterial and venous BP, and J_H, J_R, and J_E are the rates of blood loss (hemorrhage), blood gain (resuscitation), and vessel-tissue fluid exchange rate. P_A and P_V are related to V_A and V_V by arterial and venous capacitance:

$$P_A(t) - P_{A0} = K_A(V_A(t) - V_{A0}) \quad \text{(A4)}$$

$$P_V(t) - P_{V0} = K_V\big(V_V(t) - V_{V0} - (V_{VU}(t) - V_{VU0})\big) \quad \text{(A5)}$$

where P_{A0} and P_{V0} are nominal arterial and venous BP, V_{VU} is unstressed venous BV, V_{A0}, V_{V0}, V_{VU0} are nominal arterial, venous, and unstressed venous BV, and K_A and K_V are the arterial and venous elastance (reciprocal of capacitance). Total BV, V, is given by:

$$V(t) = V_A(t) + V_V(t) \quad \text{(A6)}$$

A.2. Vessel-Tissue Fluid Exchange

The vessel-tissue fluid exchange represents the resultant effect of change in BV on capillary filtration and lymphatic drainage. The fluid exchange is modeled to phenomenologically replicate the known physiological knowledge that a pre-specified fraction of blood gain and loss results in the change in BV while the remaining fraction results in the change in tissue volume. Denoting $r_B(t)$ the pre-specified change in BV in the steady state:

$$r_B(t) = \frac{1}{1+\alpha_R}\int_0^t J_R(\tau)d\tau - \frac{1}{1+\alpha_H}\int_0^t J_H(\tau)d\tau \quad \text{(A7)}$$

where α_R and α_H are the ratio with which BV and tissue volume are altered in the steady state in response to blood gain and loss, respectively. This phenomenological model was extensively validated in our prior work[56–58]. Then, the vessel-tissue fluid exchange is modeled as a simple proportional compensation:

$$J_E = K_E\big(V(t) - V_0 - r_B(t)\big) \quad \text{(A8)}$$

where V_0 is nominal BV.

A.3. Autonomic-Cardiac Regulation

The autonomic-cardiac regulation represents the control of CO and TPR to maintain arterial BP against change in BV. Established knowledge on CV physiology is modeled into simple lumped-parameter models: (i) CO is modeled to dynamically regulate the effect of perturbation in venous BP (i.e., preload), while (ii) TPR is modeled to dynamically counteract the change in arterial BP and passively react to the change in blood viscosity. In the Laplace domain:

$$\Delta Q(s) = K_C\frac{s+z_C}{s+p_C}\Delta P_V(s) \quad \text{(A9)}$$

$$\Delta R(s) = -K_R\frac{1}{s+p_R}\Delta P_A(s) + K_H\Delta H(s) \quad \text{(A10)}$$

where $\Delta Q(t) = Q(t) - Q_0$, $\Delta R(t) = R(t) - R_0$, $\Delta P_A(t) = P_A(t) - P_{A0}$, $\Delta P_V(t) = P_V(t) - P_{V0}$ with Q_0 and R_0 being nominal CO and TPR, $\Delta H(t) = H(t) - H_0$ where $H(t)$ is blood hematocrit defined as $H(t) = \frac{V_{RBC}(t)}{V_A(t)+V_V(t)}$ and H_0 is nominal blood hematocrit, K_C, K_R, and K_H are gain constants, p_C and z_C are the pole and zero associated with CO dynamics, and p_R is the pole associated with TPR dynamics.

A.4. Propofol Pharmacology and Its Integration into CV Physiology

The propofol pharmacological model consists of a 3-compartment pharmacokinetic (PK) model, an effect site delay model, and a sigmoidal pharmacodynamics (PD) model associated with BIS[33,34]. In terms of propofol mass in the central (blood) as well as fast and slow peripheral

compartments as state variables, the PK model is given by the following ordinary differential equations:

$$\dot{m}_1(t) = -(k_{10} + k_{12} + k_{13})m_1(t) + k_{21}m_2(t) + k_{31}m_3(t) + J_P(t) \quad \text{(A11)}$$

$$\dot{m}_2(t) = k_{12}m_1(t) - k_{21}m_2(t) \quad \text{(A12)}$$

$$\dot{m}_3(t) = k_{13}m_1(t) - k_{31}m_3(t) \quad \text{(A13)}$$

where m_1, m_2, and m_3 are mass in the central, fast peripheral, and slow peripheral compartments, k_{10}, k_{12}, k_{13}, k_{21}, and k_{31} are rate constants, and J_P is propofol administration rate. The effect site PD is modeled as a 1st-order dynamics with time constant k_{e0}:

$$\dot{C}_e(t) = -k_{e0}C_e(t) + \frac{V_P k_{e0} m_1(t)}{V_D(V_A(t)+V_V(t)-V_{RBC}(t))} \quad \text{(A14)}$$

where $C_e(t)$ is the effect site plasma propofol concentration, and V_D and V_P are central distribution volume (as specified in the PK model[33,34]) and nominal plasma volume in humans. In this way, the effect of varying BV ($V(t) = V_A(t) + V_V(t) - V_{RBC}(t)$) on propofol concentration is incorporated into the PD model (note that $\frac{V_D}{V_P}$ is the ratio between the central distribution volume and the actual plasma volume converting $V(t)$ to the corresponding distribution volume). Then, BIS is given by the output of a dose-response model F_{BIS} which is a function of C_e[34]:

$$BIS(t) = F_{BIS}[C_e(t)] \quad \text{(A15)}$$

In combining the CV physiology and propofol PKPD models, we made extensions to replicate the following interactions between hemorrhage resuscitation and IV sedation treatments. First, we incorporated the effect of BV change on plasma propofol concentration by making the distribution volume of the blood compartment a function of BV computed in the CV physiology model (see (A14)). Second, we incorporated the arterial vasodilation and venodilation effects of propofol by making extensions to the CV physiology model. To include the arterial vasodilation effect, we added a propofol-induced depression term to the TPR control dynamics in Eq. (A10):

$$\Delta R(s) = -K_R \frac{1}{s+p_R}\Delta P_A(s) + K_h \Delta H(s) - G_R C_e(s) \quad \text{(A16)}$$

where G_R is a gain constant associated with arterial vasodilation. To include the venodilation effect, we expressed venous BV as the sum of unstressed venous BV (V_{VU}) and stressed venous BV (V_{VS}):

$$V_V(t) = V_{VU}(t) + V_{VS}(t) \quad \text{(A17)}$$

Then, we modeled unstressed BV as a dynamical function to counteract the change in arterial BP and passively respond to the change in plasma propofol concentration:

$$\Delta V_{VU}(s) = -K_{vu} \frac{1}{s+p_R}\Delta P_A(s) + G_{VU} C_e(s) \quad \text{(A18)}$$

where $\Delta V_{VU}(t) = V_{VU}(t) - V_{VU0}$, K_{VU} is a gain constant, and G_{VU} is a gain constant associated with venodilation.

In sum, the CV physiology and propofol pharmacology parameters $\boldsymbol{\theta}_{\mathrm{CV}}$ and $\boldsymbol{\theta}_{\mathrm{PD}}$ are given by:

$$\boldsymbol{\theta}_{\mathrm{CV}} = \{\mathrm{K_A}, \mathrm{K_V}, \alpha_{\mathrm{R}}, \alpha_{\mathrm{H}}, \mathrm{K_E}, \mathrm{K_C}, \mathrm{z_C}, \mathrm{p_C}, \mathrm{K_H}, \mathrm{K_R}, \mathrm{p_R}, \mathrm{K_{vu}}, \mathrm{V_0}\} \tag{A19}$$

$$\boldsymbol{\theta}_{\mathrm{PD}} = \{\mathrm{G_R}, \mathrm{G_{VU}}\} \tag{A20}$$

Table 1: Goodness of fit of physiological model predictions with respect to in-house experimental data in terms of normalized root-mean-squared error (NRMSE).

(a) Step 1: Cardiovascular physiology model (Eq. (1))

	HCT	CO	BP
NRMSE [%]	4.9	11.9	9.9

(a) Step 2: Propofol pharmacology model (Eq. (2))

	CO	TPR	BP
NRMSE [%]	4.9	2.5	3.0

Table 2: Transient and steady-state effect of crystalloid/colloid bolus and constant-rate propofol infusion on cardiovascular (CV) variables and bispectral index (BIS).

(a) Steady state

	BP	V_{BU}	V_{BS}	CO	TPR	BIS
Crystalloid	×	×	↑	↑	↓	↑
Colloid	↑	×	↑	↑	↓	↑
Propofol	↓	×	×	×	↓	↓

(b) Transient (during and immediately after administration)

	BP	V_{BU}	V_{BS}	CO	TPR	BIS
Crystalloid	↑	↑	↑	↑	↓	↑
Colloid	↑	↑	↑	↑	↓	↑
Propofol	↓	↑	↓	↓	↓	↓

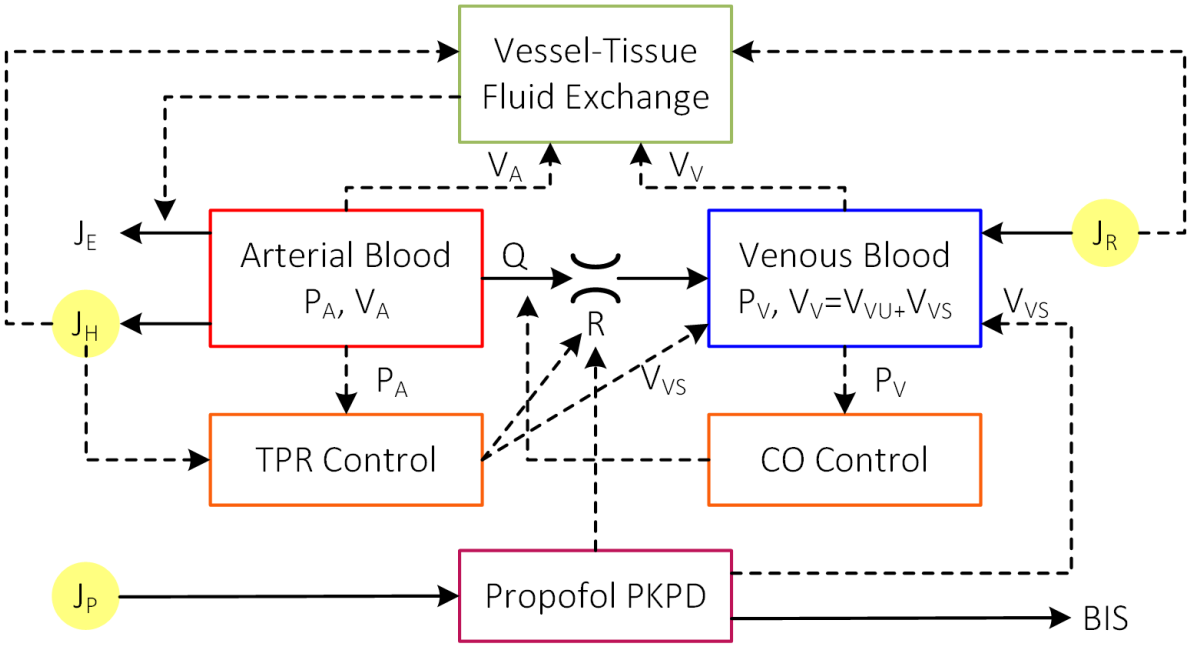

Fig. 1: A physiological model to describe the collective cardiovascular (CV) and pharmacological effects of hemorrhage resuscitation and intravenous (IV) propofol sedation treatments. Solid lines and dashed lines represent the flow of physical quantity and information, respectively. It consists of volume kinetics in the arterial and venous vessels, vessel-tissue fluid exchange, autonomic-cardiac regulation, and propofol pharmacology. P_A, P_V: arterial and venous blood pressures (BP). V_A, V_V: arterial and venous blood volumes (BV). V_{VU} and V_{VS}: unstressed and stressed venous BV. J_H, J_R, and J_P are the inputs of the physiological model: the rates of hemorrhage, hemorrhage resuscitation, and propofol infusion. Q: cardiac output (CO). R: total peripheral resistance (TPR). J_E: the rate of vessel-tissue fluid exchange.

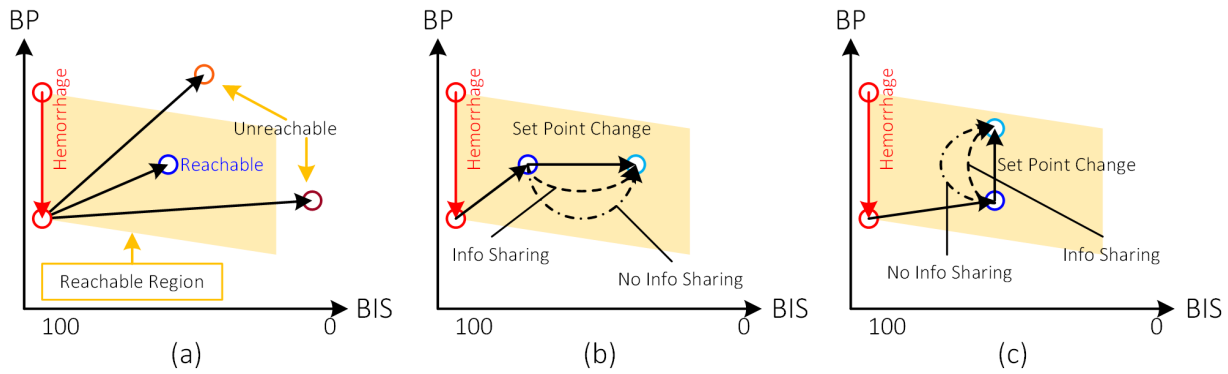

Fig. 2: Control loop interaction analysis. (a) Set point level analysis concerned the investigation of the behavior of the closed-loop controlled treatments with respect to whether the treatment set points are inside or outside the reachable region (marked in yellow background). (b)-(c): Loop level analysis concerned the investigation of the behavior of the closed-loop controlled treatments with respect to whether the resuscitation volume and propofol infusion dose changes are alerted to both treatment loops.

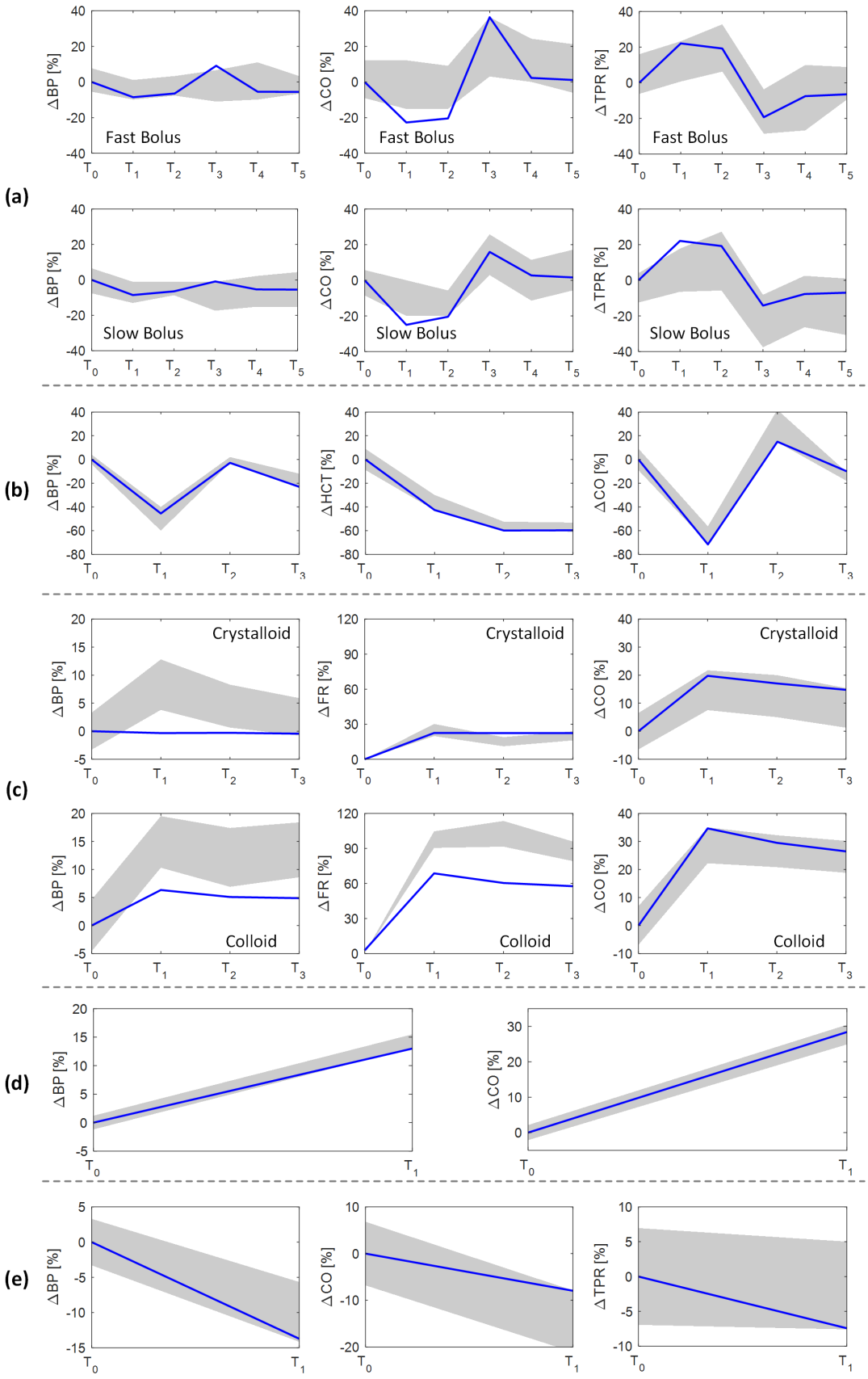
(a)
ΔBP [%]
ΔCO [%]
ΔTPR [%]
Fast Bolus
Slow Bolus
(b)
ΔBP [%]
ΔHCT [%]
ΔCO [%]
(c)
ΔBP [%]
ΔFR [%]
ΔCO [%]
Crystalloid
Colloid
(d)
ΔBP [%]
ΔCO [%]
(e)
ΔBP [%]
ΔCO [%]
ΔTPR [%]

Fig. 3: External validation of physiological model. (a) Changes in arterial BP, CO, and TPR in response to hemorrhage (15ml/kg) and crystalloid bolus (20ml/kg). T_0: pre-hemorrhage. T_1: post-hemorrhage. T_2: pre-resuscitation. T_3: post-resuscitation (0 min). T_4: post-resuscitation (60 min). T_5: post-resuscitation (120 min). Upper and lower panels show responses to fast and slow boluses. Grey range indicates 25%-75% interquartile range of the experimental responses. (b) Changes in arterial BP, HCT, and CO in response to hemorrhage titrated to 50 mmHg arterial BP and crystalloid bolus (60ml/kg). T_0: pre-hemorrhage. T_1: Hemorrhage. T_2: post-resuscitation (10 min). T_3: post-resuscitation (120 min). Grey range indicates mean+/-standard error (SE) of the experimental responses. (c) Changes in arterial BP, fluid retention, and CO in response to (upper) crystalloid (20ml/kg) bolus and (lower) colloid bolus (10ml/kg). T_0: pre-bolus. T_1: post-bolus (20 min). T_2: post-bolus (40 min). T_1: post-bolus (60 min). Grey range indicates mean+/- SE of the experimental responses. (d) Changes in arterial BP and CO in response to colloid-based volume expansion (VE). T_0: pre-VE. T_1: post-VE. Grey range indicates mean+/-SE of the experimental responses. (e) Changes in arterial BP, CO, and TPR in response to propofol administration. T_0: pre-induction. T_1: post-induction. Grey range indicates mean+/-SE of the experimental responses.

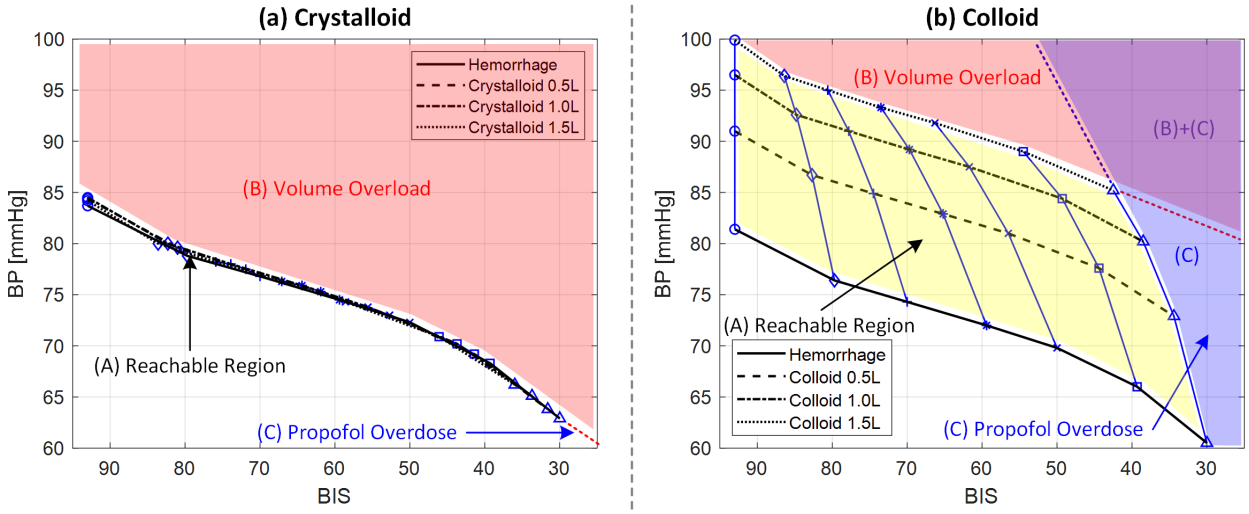

Fig. 4: Representative examples of reachable blood pressure (BP)-bispectral index (BIS) set point region in the steady state pertaining to (a) crystalloid-propofol treatments and (b) colloid-propofol treatments. Hemorrhage volume: 0.75 L. Therapeutic upper bounds: 1.5 L resuscitation volume and 0.25 mcg/kg/min propofol infusion dose (corresponding to BIS=30 in the post-hemorrhagic state).

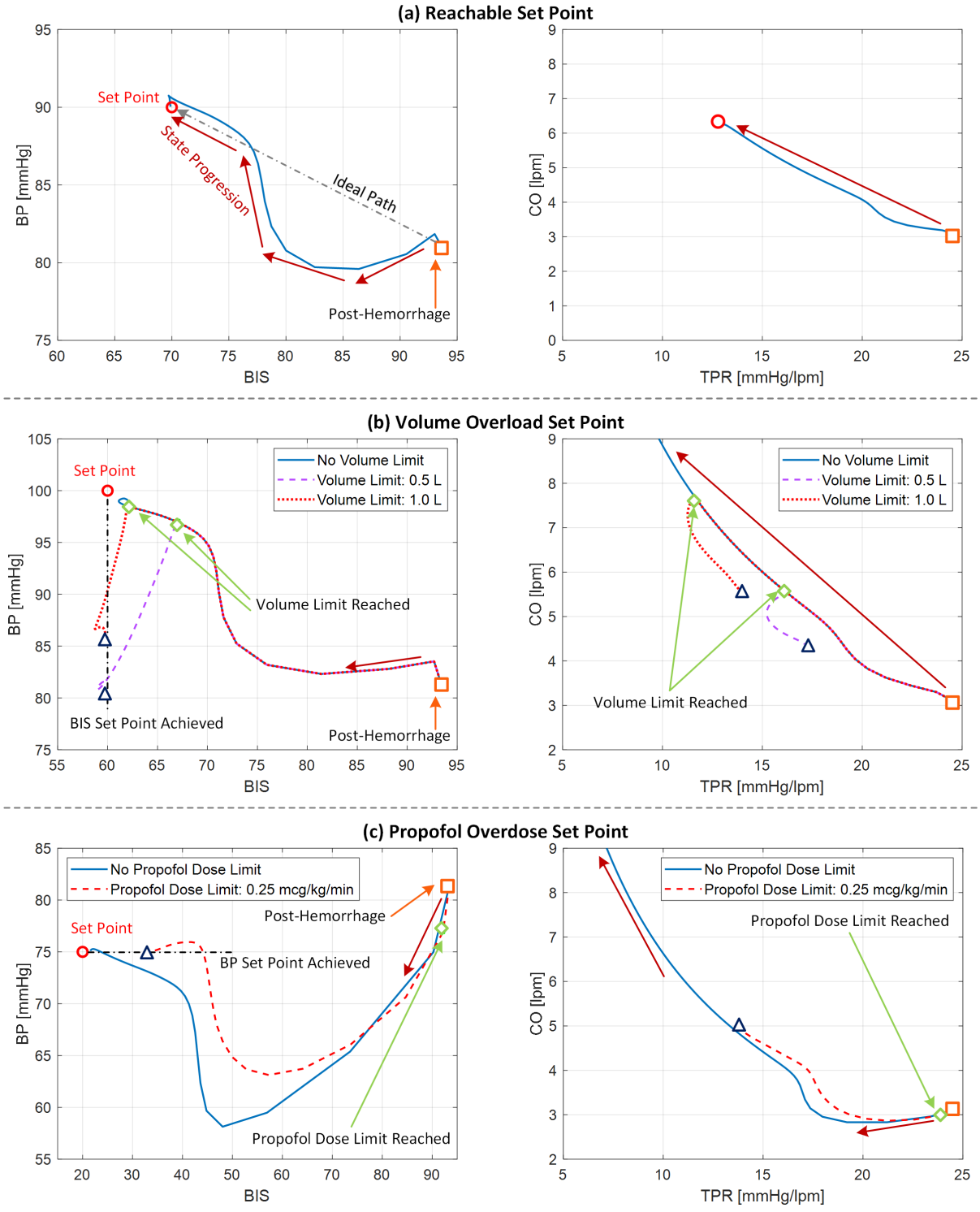

Fig. 5: Blood pressure (BP)-bispectral index (BIS) as well as cardiac output (CO)-total peripheral resistance (TPR) phase plots comparing the dynamic behavior of closed-loop controlled colloid-based hemorrhage resuscitation and propofol sedation treatments commanded to track set points in the (a) reachable region, (b) region pertaining to colloid overload, and (c) region pertaining to propofol over-dosing.

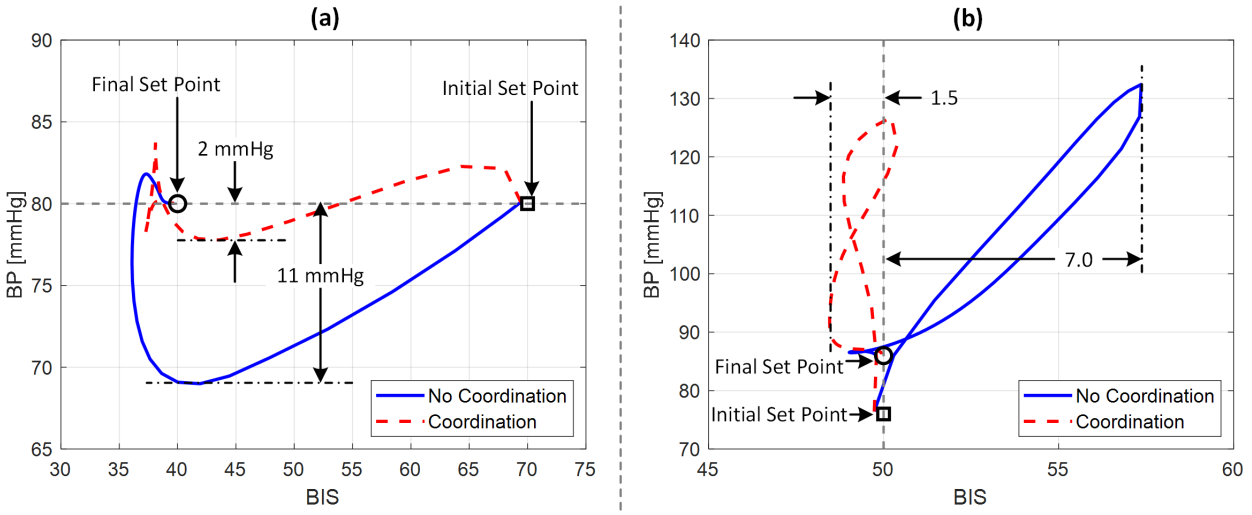

Fig. 6: Blood pressure (BP)-bispectral index (BIS) phase plots comparing the transient set point tracking behavior of closed-loop controlled colloid-based hemorrhage resuscitation and propofol sedation treatments in the absence vs. presence of information sharing between the two control loops. (a) Hemorrhage resuscitation with vs. without BIS set point change information. The initial set point is (80 mmHg, 70). BIS set point is changed to 40 via a stepwise increase in the propofol infusion dose. The maximum excursion in BP is 2 mmHg vs. 11 mmHg, and the excursion persists for 25 min. (b) IV Propofol sedation with vs. without hemorrhage resuscitation set point change information. The initial set point is (77 mmHg, 50). BP set point is changed to 86 mmHg via a resuscitation bolus. The maximum excursion in BIS is 1.5 vs. 7, and the excursion persists for 30 min.